MIMO DECOUPLING CONTROL USING A YOULA-PARAMETRIZED REGULATOR

Cs. Bányász and L. Keviczky

Széchenyi University, Győr
Computer and Automation Research Institute and Control Engineering Research Group
Hungarian Academy of Sciences
H-1111 Budapest, Kende u 13-17, HUNGARY
Phone: +361-466-5435; Fax: +361-466-7503
e-mail: banyasz@sztaki.hu ; keviczky@sztaki.hu

Abstract: It is interesting to investigate how a decoupling controller can be designed. The YOULA-parametrization is a simple method to design controllers. The KB-parametrization is a successful extension of this method for two-degree-of-freedom (*TDOF*) systems. The paper extends this methodology for multivariable case after summarizing the classical *TFM* based methods. Interesting examples are also given including a decoupling lateral control application.

Keywords: MIMO processes, YOULA-parametrization, KB-parametrization, decoupling control

1. Introduction

The state equation of *Multiple Input Multiple Output* (shortly *MIMO),* i.e., multivariable linear dynamic systems has the form

$$\frac{\mathrm{d}\boldsymbol{x}}{\mathrm{d}t} = \dot{\boldsymbol{x}} = \mathbf{A}\,\boldsymbol{x} + \mathbf{B}\,\boldsymbol{u} \qquad\qquad (1)$$
$$\boldsymbol{y} = \mathbf{C}\,\boldsymbol{x} + \mathbf{D}\,\boldsymbol{u}$$

where $\mathbf{A}$, $\mathbf{B}$, $\mathbf{C}$ and $\mathbf{D}$ are ($n \times n$), ($n \times p$), ($p \times n$) and ($p \times p$) matrices, respectively. For the simplicity, let the number of the input and output variables be the same and denote by p (quadratic systems), so the input $\boldsymbol{u}$ and the output $\boldsymbol{y}$ are p-dimensional vectors. The ($n \times n$)-dimensional *transfer function matrix* (*TFM*) of the *MIMO* process is

$$\boldsymbol{P}(s) = \mathbf{C}(s\,\mathbf{I} - \mathbf{A})^{-1}\,\mathbf{B} + \mathbf{D} = \mathbf{C}\,\boldsymbol{\Phi}(s)\,\mathbf{B} + \mathbf{D} = \frac{1}{\mathcal{A}(s)}\mathcal{B}(s) \qquad (2)$$

where

$$\boldsymbol{\Phi}(s) = (s\mathbf{I} - \mathbf{A})^{-1} = \frac{1}{\mathcal{A}(s)}\boldsymbol{\Psi}(s) \quad \text{and} \quad \boldsymbol{\Psi}(s) = \mathbf{adj}(s\mathbf{I} - \mathbf{A}) \qquad (3)$$

The scalar denominator

$$\mathcal{A}(s) = \det(s\mathbf{I} - \mathbf{A}) \qquad (4)$$

is the n-th-degree characteristic polynomial of the process. $\boldsymbol{\Phi}$ and $\boldsymbol{\Psi}$ are also ($n \times n$)-dimensional. The form (2) means the simplest *MIMO* process model, though $\boldsymbol{P}(s)$ is not necessarily minimal, it might be reduced. The right side of (2) is usually also called the "naive" model of the *MIMO* process. (In this paper the parameter matrices of the state equation are denoted by bold plain fonts while the cursive bold fonts denote the *TFM*s.)

At the control design of the *SISO* processes the decomposition of the process into inverse stable and unstable factors was usually a requirement. The *TFM* $\boldsymbol{P}$ of a *MIMO* process can be decomposed in a similar way

$$\boldsymbol{P} = \boldsymbol{P}_{-}\boldsymbol{P}_{+} \neq \boldsymbol{P}_{+}\boldsymbol{P}_{-} \tag{5}$$

where $\boldsymbol{P}_{+}$ and $\boldsymbol{P}_{-}$ are the inverse stable (*IS*) and inverse unstable (*IU*) matrix operators (*TFM*), respectively. Obviously $\boldsymbol{P}$ can be always written in the equivalent form

$$\boldsymbol{P} = \overline{\boldsymbol{P}}_{+}\overline{\boldsymbol{P}}_{-} \neq \overline{\boldsymbol{P}}_{-}\overline{\boldsymbol{P}}_{+} \tag{6}$$

2. The YOULA-parametrized *MIMO* closed control loop

Formally it is very easy to extend the YOULA-parametrization to *MIMO* processes by introducing the *TFM*

$$\boldsymbol{Q} = \boldsymbol{C}(\mathbf{I} - \boldsymbol{PC})^{-1} = (\mathbf{I} - \boldsymbol{CP})^{-1}\boldsymbol{C} \tag{7}$$

which results in the following *YP MIMO* regulator [6], [7]

$$\boldsymbol{C} = (\mathbf{I} - \boldsymbol{QP})^{-1}\boldsymbol{Q} = \boldsymbol{Q}(\mathbf{I} - \boldsymbol{PQ})^{-1} \tag{8}$$

Here $\boldsymbol{P}$ is assumed to be stable. It can be easily verified that the two sides of (7) and (8) are the same.

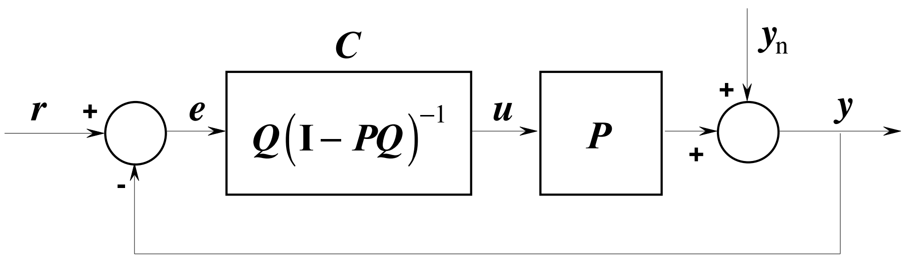

Figure 1. The generalization of the YOULA-parametrization for *MIMO* processes

The following identities have important role in the investigation of the *TFM* of the *MIMO* closed control loop

$$\begin{aligned} (\mathbf{I} + \boldsymbol{PC})^{-1} &= \left[\mathbf{I} + \boldsymbol{PQ}(\mathbf{I} - \boldsymbol{PQ})^{-1}\right]^{-1} = \mathbf{I} - \boldsymbol{PQ} \\ (\mathbf{I} + \boldsymbol{CP})^{-1} &= \left[\mathbf{I} + (\mathbf{I} - \boldsymbol{QP})^{-1}\boldsymbol{QP}\right]^{-1} = \mathbf{I} - \boldsymbol{QP} \end{aligned} \tag{9}$$

$$\left[\mathbf{I} + (\mathbf{I} - \mathbf{A})^{-1}\mathbf{A}\right]^{-1} = \mathbf{I} - \mathbf{A} \quad \text{and} \quad \left[\mathbf{I} + \mathbf{B}(\mathbf{I} - \mathbf{B})^{-1}\right]^{-1} = \mathbf{I} - \mathbf{B} \tag{10}$$

The overall transfer characteristics of the *YP* closed system shown in Fig. 1 can be obtained by simple calculations

$$y = PQr + (\mathbf{I} - PQ)\, y_n \tag{11}$$

but it has to be taken into account that the multiplication of the *TFM* is not commutative. Here the *KB*-parametrization introduced at *SISO* processes can also be applied, thus the multiplication by the pre-filter Q^{-1}, what results in the *TDOF MIMO* closed system of Fig. 2, where the overall transfer characteristic is

$$y = Pr + (\mathbf{I} - PQ)\, y_n \tag{12}$$

what virtually opens the closed-loop. Note that the *KB*-parametrization can be applied for all closed control loops, not only for the *YP* loops and it always virtually opens the loop, thus it ensures the tracking properties Pr. The noise rejection property $(\mathbf{I} - PQ)$, however, appears only in the case of *YP*.

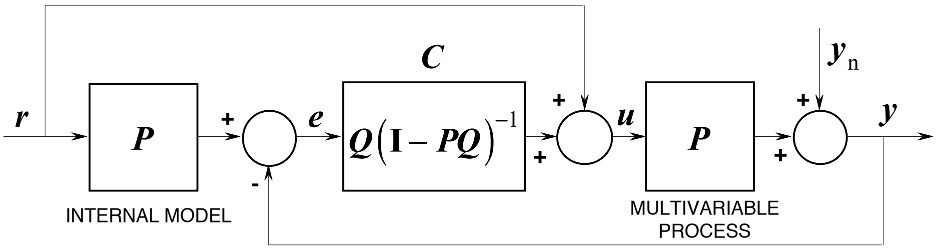

Figure 2. The *KB*-parametrized *MIMO* closed control loop

Extending the *generic TDOF* closed system from the *SISO* processes [6] to *MIMO* processes [7], we get the closed-loop shown in Fig. 3.

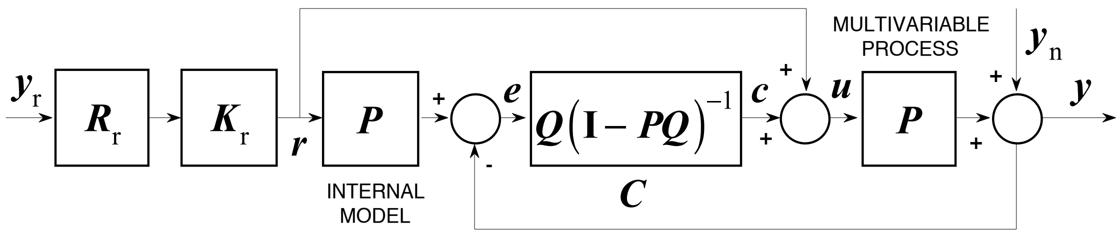

Figure 3. *Generic TDOF* closed-loop of *MIMO* processes

The overall characteristic of the generic closed system is

$$y = PQ_r\, y_r + (I - PQ_n)\, y_n = PK_r R_r\, y_r + (I - PK_n R_n)\, y_n = y_t + y_d \tag{13}$$

Assume that the stable *MIMO* process P can be decomposed according to (5). Then the *MIMO* YOULA-parameters are

$$Q = Q_n = K_n R_n = P_+^{-1} G_n R_n \tag{14}$$

and

$$Q_r = K_r R_r = P_+^{-1} G_r R_r \quad ; \quad K_n = P_+^{-1} G_n \quad ; \quad K_r = P_+^{-1} G_r \tag{15}$$

The YOULA-parametrized *MIMO* regulator is

$$\boldsymbol{C} = \boldsymbol{Q}(\mathbf{I} - \boldsymbol{P}\boldsymbol{Q})^{-1} = \boldsymbol{K}_\mathrm{n}\boldsymbol{R}_\mathrm{n}(\mathbf{I} - \boldsymbol{P}\boldsymbol{K}_\mathrm{n}\boldsymbol{R}_\mathrm{n})^{-1} = \boldsymbol{P}_+^{-1}\boldsymbol{G}_\mathrm{n}\boldsymbol{R}_\mathrm{n}(\mathbf{I} - \boldsymbol{P}_-\boldsymbol{G}_\mathrm{n}\boldsymbol{R}_\mathrm{n})^{-1} \tag{16}$$

Using the expressions (14)-(16), the obtained closed system has the form

$$\boldsymbol{y} = \boldsymbol{P}_-\boldsymbol{G}_\mathrm{r}\boldsymbol{R}_\mathrm{r}\,\boldsymbol{y}_\mathrm{r} + (\mathbf{I} - \boldsymbol{P}_-\boldsymbol{G}_\mathrm{n}\boldsymbol{R}_\mathrm{n})\,\boldsymbol{y}_\mathrm{n} = \boldsymbol{y}_\mathrm{t} + \boldsymbol{y}_\mathrm{d} \tag{17}$$

where, similarly to the *SISO* case, $\boldsymbol{y}_\mathrm{t}$ and $\boldsymbol{y}_\mathrm{d}$ mean the tracking and disturbance rejection properties, respectively. Here $\boldsymbol{K}_\mathrm{r}$ and $\boldsymbol{K}_\mathrm{n}$ contain the inverse $\boldsymbol{P}_+^{-1}$ of the invertible part $\boldsymbol{P}_+$ of $\boldsymbol{P}$, furthermore $\boldsymbol{G}_\mathrm{r}$ and $\boldsymbol{G}_\mathrm{n}$ attenuate the effect of the invariant factor $\boldsymbol{P}_-$.

If the process $\boldsymbol{P}$ is decomposed according to (6), then we get the YOULA-parametrized *MIMO* regulator as

$$\bar{\boldsymbol{C}} = (\mathbf{I} - \bar{\boldsymbol{Q}}\bar{\boldsymbol{P}})^{-1}\bar{\boldsymbol{Q}} = (\mathbf{I} - \boldsymbol{R}_\mathrm{n}\bar{\boldsymbol{K}}_\mathrm{n}\bar{\boldsymbol{P}})^{-1}\boldsymbol{R}_\mathrm{n}\bar{\boldsymbol{K}}_\mathrm{n} = (\mathbf{I} - \boldsymbol{R}_\mathrm{n}\bar{\boldsymbol{G}}_\mathrm{n}\bar{\boldsymbol{P}}_-)^{-1}\boldsymbol{R}_\mathrm{n}\bar{\boldsymbol{G}}_\mathrm{n}\bar{\boldsymbol{P}}_+^{-1} \tag{18}$$

where

$$\bar{\boldsymbol{K}}_\mathrm{n} = \bar{\boldsymbol{G}}_\mathrm{n}\,\bar{\boldsymbol{P}}_+^{-1} \tag{19}$$

Now the equation of the closed system becomes

$$\boldsymbol{y} = \boldsymbol{P}_-\boldsymbol{G}_\mathrm{r}\boldsymbol{R}_\mathrm{r}\,\boldsymbol{y}_\mathrm{r} + (\mathbf{I} - \boldsymbol{R}_\mathrm{n}\bar{\boldsymbol{G}}_\mathrm{n}\bar{\boldsymbol{P}}_-)\,\boldsymbol{y}_\mathrm{n} = \boldsymbol{y}_\mathrm{t} + \bar{\boldsymbol{y}}_\mathrm{d} \tag{20}$$

It is well seen that the tracking property $\boldsymbol{y}_\mathrm{t}$ is the same for the two-type of the decomposition, the noise rejection properties $\boldsymbol{y}_\mathrm{d}$ and $\bar{\boldsymbol{y}}_\mathrm{d}$, however, may be different.

Note that while, for the *SISO* case, the realizability of the YOULA-parametrized regulator can be simply ensured by the reasonable choice of the pole access of the reference models R_r and R_n, the same cannot be stated for the *MIMO* case. It is true that in many cases, raising the pole access of the elements in the main diagonal of $\boldsymbol{R}_\mathrm{r}$ and $\boldsymbol{R}_\mathrm{n}$ helps the realizability, if they are given in *TFM* form. The general condition, however, always needs further, thorough investigation. Consider next some special cases.

The YOULA-parametrized MIMO regulator for the "naive" process model

The derivation of the regulators (16) and (18) requires complex operations between the *TFM*s. This computation demand can be slightly decreased by using the "naive" model given in (2). In this case the decomposition (5) has the form

$$\boldsymbol{P}(s) = \boldsymbol{P}_-\boldsymbol{P}_+ = \frac{1}{\mathcal{A}(s)}\mathcal{B}(s) = \frac{1}{\mathcal{A}(s)}\mathcal{B}_-(s)\mathcal{B}_+(s) \tag{21}$$

The advantage of this model is that the designated operation with the polynomial $\mathcal{A}(s)$ in the denominator can be exchanged by any matrix polynomial. Futher simplification can be reached for inverse stable processes, when the model (2) is

$$\boldsymbol{P} = \frac{1}{\mathcal{A}(s)}\mathcal{B}_{+}(s) \quad ; \quad \mathcal{B}_{+}=\mathcal{B} \quad ; \quad \mathcal{B}_{-}=\mathbf{I} \tag{22}$$

Let the reference models be given in the "naive" form, i.e.,

$$\boldsymbol{R}_{\mathrm{r}} = \frac{1}{\mathcal{A}_{\mathrm{r}}(s)}\mathcal{B}_{\mathrm{r}}(s) \quad \text{and} \quad \boldsymbol{R}_{\mathrm{n}} = \frac{1}{\mathcal{A}_{\mathrm{n}}(s)}\mathcal{B}_{\mathrm{n}}(s) \tag{23}$$

If $\mathcal{B}_{-}=\mathbf{I}$ and $\mathcal{B}_{+}=\mathcal{B}$, then further optimization is impossible, thus it is reasonable to choose $\boldsymbol{G}_{\mathrm{r}} = \boldsymbol{G}_{\mathrm{n}} = \mathbf{I}$. In this case the *MIMO* YOULA-parameter is

$$\boldsymbol{Q} = \boldsymbol{Q}_{\mathrm{n}} = \mathcal{A}(s)\mathcal{B}^{-1}(s)\boldsymbol{R}_{\mathrm{n}} = \frac{\mathcal{A}(s)}{\mathcal{A}_{\mathrm{n}}(s)}\mathcal{B}^{-1}(s)\mathcal{B}_{\mathrm{n}}(s) \tag{24}$$

and the YOULA-parametrized *MIMO* regulator becomes

$$\boldsymbol{C}(s) = \mathcal{A}(s)\mathcal{B}^{-1}(s)\boldsymbol{R}_{\mathrm{n}}(s)\left[\mathbf{I} - \boldsymbol{R}_{\mathrm{n}}(s)\right]^{-1} = \mathcal{A}(s)\mathcal{B}_{+}^{-1}(s)\mathcal{B}_{\mathrm{n}}(s)\left[\mathcal{A}_{\mathrm{n}}(s)\mathbf{I} - \mathcal{B}_{\mathrm{n}}(s)\right]^{-1} \tag{25}$$

Sampled data systems

In many practical cases the *MIMO* process model is given in a special, inverse stable form. This is especially valid for sampled (or discrete-time: DT) processes

$$\boldsymbol{G} = \boldsymbol{G}_{-}\boldsymbol{G}_{+} = z^{-d}\boldsymbol{G}_{+} = \bar{\boldsymbol{G}}_{+}\bar{\boldsymbol{G}}_{-} = \bar{\boldsymbol{G}}_{+}z^{-d} \quad ; \quad \boldsymbol{G}_{+} = \bar{\boldsymbol{G}}_{+} \tag{26}$$

Here for all inputs in the main diagonal the time-delay is z^{-d}. All other variants can be taken into account in $\boldsymbol{G}_{+}$. In this case the YOULA-parameter is

$$\boldsymbol{Q} = \boldsymbol{G}_{+}^{-1}\boldsymbol{R}_{\mathrm{n}} \quad ; \quad \bar{\boldsymbol{Q}} = \boldsymbol{R}_{\mathrm{n}}\bar{\boldsymbol{G}}_{+}^{-1} \tag{27}$$

Using these parameters the regulator (16) and (18) becomes

$$\begin{aligned} \boldsymbol{C} &= \boldsymbol{Q}(\mathbf{I} - \boldsymbol{P}\boldsymbol{Q})^{-1} = \boldsymbol{G}_{+}^{-1}\boldsymbol{R}_{\mathrm{n}}\left(\mathbf{I} - \boldsymbol{R}_{\mathrm{n}}z^{-d}\right)^{-1} = \boldsymbol{G}_{+}^{-1}\left(\mathbf{I} - \boldsymbol{R}_{\mathrm{n}}z^{-d}\right)^{-1}\boldsymbol{R}_{\mathrm{n}} \\ \bar{\boldsymbol{C}} &= \left(\mathbf{I} - \bar{\boldsymbol{Q}}\bar{\boldsymbol{P}}\right)^{-1}\bar{\boldsymbol{Q}} = \left(\mathbf{I} - \boldsymbol{R}_{\mathrm{n}}z^{-d}\right)^{-1}\boldsymbol{R}_{\mathrm{n}}\boldsymbol{G}_{+}^{-1} = \boldsymbol{R}_{\mathrm{n}}\left(\mathbf{I} - \boldsymbol{R}_{\mathrm{n}}z^{-d}\right)^{-1}\boldsymbol{G}_{+}^{-1} \end{aligned} \tag{28}$$

Here $\boldsymbol{G}_{+} = \bar{\boldsymbol{G}}_{+}$ is considered and the identity

$$\boldsymbol{R}_{\mathrm{n}}\left(\mathbf{I} - \boldsymbol{R}_{\mathrm{n}}z^{-d}\right)^{-1} = \left(\mathbf{I} - \boldsymbol{R}_{\mathrm{n}}z^{-d}\right)^{-1}\boldsymbol{R}_{\mathrm{n}} \tag{29}$$

can be simply checked. The closed system for the two-type of regulators are exactly the same

$$\begin{aligned} \boldsymbol{y} &= \boldsymbol{R}_{\mathrm{r}}z^{-d}\boldsymbol{y}_{\mathrm{r}} + \left(\mathbf{I} - \boldsymbol{R}_{\mathrm{n}}z^{-d}\right)\boldsymbol{y}_{\mathrm{n}} = \boldsymbol{y}_{\mathrm{t}} + \boldsymbol{y}_{\mathrm{d}} \\ \boldsymbol{y} &= \boldsymbol{R}_{\mathrm{r}}z^{-d}\boldsymbol{y}_{\mathrm{r}} + \left(\mathbf{I} - \boldsymbol{R}_{\mathrm{n}}z^{-d}\right)\boldsymbol{y}_{\mathrm{n}} = \boldsymbol{y}_{\mathrm{t}} + \bar{\boldsymbol{y}}_{\mathrm{d}} \end{aligned} \tag{30}$$

thus $\boldsymbol{y}_{\mathrm{d}} = \bar{\boldsymbol{y}}_{\mathrm{d}}$. Note that for this case $\boldsymbol{G}_{\mathrm{r}} = \boldsymbol{G}_{\mathrm{n}} = \mathbf{I}$ is chosen, since the effect of the invariant factor $\boldsymbol{G}_{-} = z^{-d}\mathbf{I}$ cannot be attenuated.

The DT "naive" model of the *MIMO* process is

$$\boldsymbol{G}(z) = \frac{1}{\mathcal{A}(z)}\mathcal{B}(z) \quad ; \quad \mathcal{B}_{+} = \mathcal{B} \quad ; \quad \mathcal{B}_{-} = z^{-d}\mathbf{I} \tag{31}$$

and the sampled YOULA-parametrized *MIMO* regulator is obtained by performing the analogous computations providing (25)

$$\begin{aligned}\boldsymbol{C}(z) &= \mathcal{A}(z)\mathcal{B}^{-1}(z)\mathcal{B}_{\mathrm{n}}(z)\left[\mathcal{A}_{\mathrm{n}}(z)\mathbf{I} - z^{-d}\mathcal{B}_{\mathrm{n}}(z)\right]^{-1} = \\ &= \mathcal{A}(z)\mathcal{B}_{+}^{-1}(z)\mathcal{B}_{\mathrm{n}}(z)\left[\mathcal{A}_{\mathrm{n}}(z)\mathbf{I} - z^{-d}\mathcal{B}_{\mathrm{n}}(z)\right]^{-1}\end{aligned} \tag{32}$$

It is worth to check that the similarly computed sampled YOULA-parametrized *SISO* regulator has the form

$$C = \mathcal{A}(z)B^{-1}(z)B_{\mathrm{n}}(z)\left[\mathcal{A}_{\mathrm{n}}(z) - z^{-d}B_{\mathrm{n}}(z)\right]^{-1} = \mathcal{A}(z)B_{+}^{-1}(z)B_{\mathrm{n}}(z)\left[\mathcal{A}_{\mathrm{n}}(z) - z^{-d}B_{\mathrm{n}}(z)\right]^{-1} \tag{33}$$

In these expressions the reference model has also the "naive" form. Let us assume now that $\boldsymbol{R}_{\mathrm{n}}$ is given in left side *MFD* form, i.e.,

$$\boldsymbol{R}_{\mathrm{n}} = \mathcal{A}_{\mathrm{n}}^{-1}(z)\mathcal{B}_{\mathrm{n}}(z) = \left[\mathbf{I} + \tilde{\mathcal{A}}_{\mathrm{n}}\left(z^{-1}\right)\right]^{-1}\mathcal{B}_{\mathrm{n}}\left(z^{-1}\right) \tag{34}$$

In this case the output of the regulator can be computed by a two-step algorithm. Let us denote the output by the vector $\boldsymbol{c}[k]$. It is reasonable to use (18) according to which the necessary computation has the form

$$\boldsymbol{c} = \bar{\boldsymbol{C}}\boldsymbol{e} = \left(\mathbf{I} - \boldsymbol{R}_{\mathrm{n}}\bar{\boldsymbol{G}}_{-}\right)^{-1}\boldsymbol{R}_{\mathrm{n}}\bar{\boldsymbol{G}}_{+}^{-1}\boldsymbol{x} \quad ; \quad \boldsymbol{x} = \bar{\boldsymbol{G}}_{+}^{-1}\boldsymbol{e} \tag{35}$$

Here the auxiliary variable $\boldsymbol{x}[k]$ is introduced. Using these equations the regulator can be written in the form of vector difference equation form linear in parameters

$$\boldsymbol{c} = \left(\mathcal{B}_{\mathrm{n}}\mathcal{N}_{\mathrm{L}}^{-} - \tilde{\mathcal{A}}_{\mathrm{n}}\right)\boldsymbol{c} + \mathcal{B}_{\mathrm{n}}\boldsymbol{x} \tag{36}$$

where $\boldsymbol{x}[k]$ can also be given in similar form

$$\boldsymbol{x} = \mathcal{D}_{\mathrm{L}}\,\boldsymbol{e} - \tilde{\mathcal{N}}_{\mathrm{L}}^{+}\boldsymbol{x} \tag{37}$$

In the equations of the regulator the following simple notations are used

$$\bar{\boldsymbol{G}}_{+}^{-1} = \left[\mathcal{N}_{\mathrm{L}}^{+}(z)\right]^{-1}\mathcal{D}_{\mathrm{L}}(z) \quad ; \quad \bar{\boldsymbol{G}}_{-} = \mathcal{N}_{\mathrm{L}}^{-} \quad ; \quad \mathcal{N}_{\mathrm{L}}^{+} = \mathbf{I} + \tilde{\mathcal{N}}_{\mathrm{L}}^{+} \tag{38}$$

3. Decoupling control of the *MIMO* process models

The decoupling control of *M*ulti-*I*nput-*M*ulti-*O*utput (*MIMO*) processes is not a simple problem. In general case, considering *MIMO* process models, each input signal has effect on each output signal. The same is valid for the all elements of the output disturbance. It is an important practical task to construct control system where each reference signal has effect only on the corresponding output signal. Similarly it is a favorable case when a certain output disturbance has effect on a given output signal and has no effect at all on the other outputs. The joint solutions of the above tasks are called decoupling or decoupling control. The practical solutions available in the literature usually apply two approaches [12], [14], [15].

The first approach applies state feedback where the decoupling vector can be chosen by algebraic method in order to reach partial or complete decoupling. These methods are very complicated, do not illustrate well how the decoupling operates, therefore they are not widely used in the engineering practice [14].

The other approach introduces process model structures (*P* and *V* structures) what handle the feed-forward and feedback elements of the *TFM* separately. The analysis of these elements makes easier the design of the necessary control though they do not provide systematic solution and do not give the theoretical limits of the decoupling [14].

Let us investigate the decoupling for sampled systems where the *TFM* of the process is assumed as

$$\boldsymbol{G} = \boldsymbol{G}_{\mathrm{D}} + \boldsymbol{G}_{\mathrm{A}} = \boldsymbol{G}_{\mathrm{D}}\left(\boldsymbol{I} + \boldsymbol{G}_{\mathrm{D}}^{-1}\boldsymbol{G}_{\mathrm{A}}\right) = \left(\boldsymbol{I} + \boldsymbol{G}_{\mathrm{A}}\boldsymbol{G}_{\mathrm{D}}^{-1}\right)\boldsymbol{G}_{\mathrm{D}} \tag{39}$$

Here $\boldsymbol{G}_{\mathrm{D}}$ contains the diagonal elements, i.e., it is a diagonal matrix, $\boldsymbol{G}_{\mathrm{A}}$ does the elements outside the diagonal (antidiagonal elements) in the original structure. The block scheme of the *MIMO* processes is usually feed-forward like as it is shown on Fig. 4 for two-variable case. The operation of the decoupling regulators is usually demonstrated on two-input two-output simple *MIMO* systems where the essence of the method can be understood in the simplest way. In the industrial practice the input and output variables are usually considered in pairs if the technology allows. These kinds of schema are used next to illustrate the methods.

The decoupler, serially connected with the *MIMO* process and providing the decoupling effect, is noted by $\boldsymbol{D}$. One of the most natural decoupling could be reached by the compensator $\boldsymbol{D} = \boldsymbol{D}_{\mathrm{o}} = \boldsymbol{G}^{-1}$, i.e., by the inverse of the process, what would mean complete decoupling $\boldsymbol{D}_{\mathrm{o}}\boldsymbol{G} = \boldsymbol{I}$. But the inverse is usually not realisable and there is almost never need to eliminate the complete dynamics of the process. In general case the structure of the decoupler $\boldsymbol{D}$ corresponds to the process model shown on Fig. 4 if the elements G_{ij} are simply substituted by D_{ij}.

Considering the engineering aspects the ideal decoupling would contain the process dynamics $\boldsymbol{G}_{\mathrm{D}}$ in the main diagonal what could be reached by the following compensator

$$\boldsymbol{D} = \boldsymbol{D}_{\mathrm{i}} = \boldsymbol{G}^{-1}\boldsymbol{G}_{\mathrm{D}} \tag{40}$$

Observe that this case also requires the inverse of the process though in certain cases there are more chances to realize the elements of the product $\boldsymbol{G}^{-1}\boldsymbol{G}_{\mathrm{D}}$ than those of $\boldsymbol{G}^{-1}$.

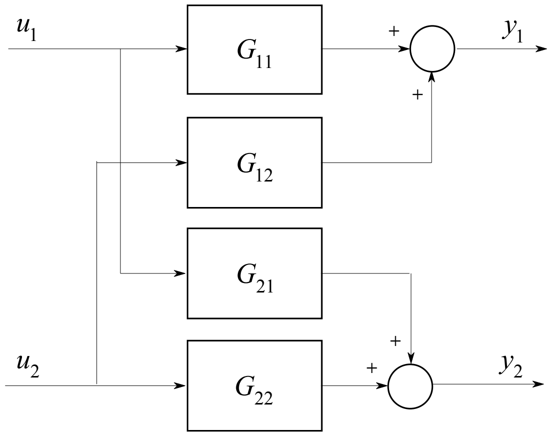

Figure 4. Block scheme of two-variable *MIMO* process

There are models for decoupling where the feed-forward and feedback effects appear mixed. Such topology is shown in Fig. 5. This structure is called V-topology or inverse (inverted) structure [12], [15].

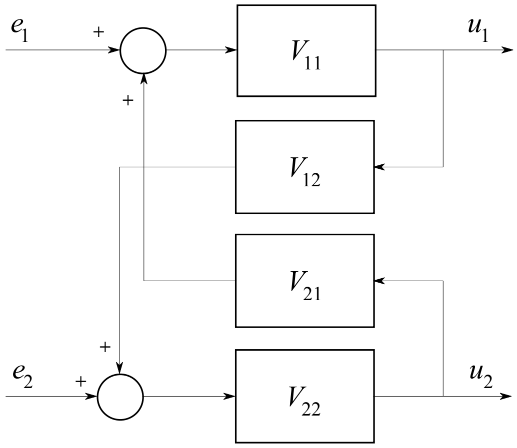

Figure 5. Block scheme of the decoupler of V-topology

The relationships of the resulting model can be written as

$$\begin{bmatrix} u_1 \\ u_2 \end{bmatrix} = \begin{bmatrix} V_{11} & 0 \\ 0 & V_{22} \end{bmatrix} \begin{bmatrix} e_1 \\ e_2 \end{bmatrix} + \begin{bmatrix} V_{11} & 0 \\ 0 & V_{22} \end{bmatrix} \begin{bmatrix} 0 & V_{12} \\ V_{21} & 0 \end{bmatrix} \begin{bmatrix} u_1 \\ u_2 \end{bmatrix} \tag{41}$$

Analogously with the notations introduced in (39) we can write now that

$$\boldsymbol{u} = \boldsymbol{V}_{\mathrm{D}}\, \boldsymbol{e} + \boldsymbol{V}_{\mathrm{D}}\, \boldsymbol{V}_{\mathrm{A}}\, \boldsymbol{u} \tag{42}$$

where the decomposition

$$\boldsymbol{V} = \boldsymbol{V}_{\mathrm{D}} + \boldsymbol{V}_{\mathrm{A}} \tag{43}$$

for diagonal and antidiagonal components is similar what was used for the process model. Based on (39) we can write that

$$\boldsymbol{u} = \left(\boldsymbol{I} - \boldsymbol{V}_\mathrm{D}\,\boldsymbol{V}_\mathrm{A}\right)^{-1} \boldsymbol{V}_\mathrm{D}\,\boldsymbol{e} = \boldsymbol{D}_\mathrm{V}\,\boldsymbol{e} \tag{44}$$

The V-topology can be simply used for the design of a decoupling compensator. Let us use the following equation for the design of the decoupling

$$\boldsymbol{G}\,\boldsymbol{D}_\mathrm{V} = \boldsymbol{G}_\mathrm{D}\left(\boldsymbol{I} + \boldsymbol{G}_\mathrm{D}^{-1}\,\boldsymbol{G}_\mathrm{A}\right)\left(\boldsymbol{I} - \boldsymbol{V}_\mathrm{D}\,\boldsymbol{V}_\mathrm{A}\right)^{-1} \boldsymbol{V}_\mathrm{D} \tag{45}$$

Observe that if in the decoupler $\boldsymbol{V}_\mathrm{D}\,\boldsymbol{V}_\mathrm{A} = -\boldsymbol{G}_\mathrm{D}^{-1}\,\boldsymbol{G}_\mathrm{A}$ is chosen then the ideal decoupling $\boldsymbol{G}\,\boldsymbol{D}_\mathrm{V} = \boldsymbol{G}_\mathrm{D}\,\boldsymbol{V}_\mathrm{D}$ is ensured. It can be stated that the elements of $\boldsymbol{V}_\mathrm{D}$ can provide the decoupled, already single variable regulator in the control loop. The realization of the above compensation is ensured by the following choices

$$\boldsymbol{V}_\mathrm{A} = -\boldsymbol{G}_\mathrm{A} \quad ; \quad \boldsymbol{V}_\mathrm{D} = \boldsymbol{G}_\mathrm{D}^{-1} \tag{46}$$

These relationships explain the introduction of the V-topology since the prescribed operations are so simple that they can be performed manually.

Using the design relationships (46) it can be seen that the V-topology shown here corresponds to the following decoupling compensator

$$\boldsymbol{D}_\mathrm{V} = \boldsymbol{G}^{-1}\,\boldsymbol{G}_\mathrm{D}\,\boldsymbol{V}_\mathrm{D} \tag{47}$$

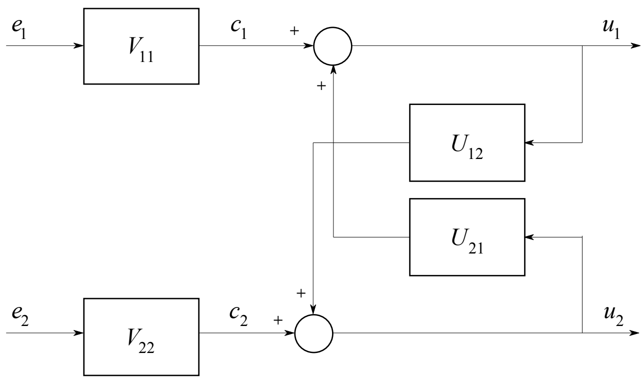

Figure 6. Block scheme of the decoupler of the U-topology

The practice of the decoupling tasks inspired the introduction of a very useful structure what can be seen in the right side of the Fig. 6 between the variables $\boldsymbol{c}$ and $\boldsymbol{u}$. Let us call this U-topology where U (unity) refers to the channels having unity transfer. It is well seen from the comparison with the V-topology that the U-topology can be obtained by the choices $U_{11} = 1$ and $U_{22} = 1$, thus corresponds to $\boldsymbol{V}_\mathrm{D} = \boldsymbol{I}$. Let us write $\boldsymbol{D}_\mathrm{U}$ for this case and substituting $\boldsymbol{V}_\mathrm{D} = \boldsymbol{I}$ into $\boldsymbol{D}_\mathrm{V}$ we get

$$\boldsymbol{D}_\mathrm{U} = \boldsymbol{D}_\mathrm{V}\big|_{\boldsymbol{V}_\mathrm{D}=\boldsymbol{I}} = \left(\boldsymbol{I} - \boldsymbol{U}_\mathrm{A}\right)^{-1} \tag{48}$$

Here it is assumed that, in comply with the notations of (39) and (43), $\boldsymbol{U} = \boldsymbol{I} + \boldsymbol{U}_\mathrm{A}$. After identical rearrangements we get

$$\boldsymbol{D}_{\mathrm{U}} = \left(\boldsymbol{I} - \boldsymbol{U}_{\mathrm{A}}\right)^{-1} = \left[\boldsymbol{G}_{\mathrm{D}}\left(\boldsymbol{I} - \boldsymbol{U}_{\mathrm{A}}\right)\right]^{-1} \boldsymbol{G}_{\mathrm{D}} = \left(\boldsymbol{G}_{\mathrm{D}} - \boldsymbol{G}_{\mathrm{D}}\boldsymbol{U}_{\mathrm{A}}\right)^{-1} \boldsymbol{G}_{\mathrm{D}} \tag{49}$$

It is clearly seen that choosing $\boldsymbol{U}_{\mathrm{A}} = -\boldsymbol{G}_{\mathrm{D}}^{-1}\boldsymbol{G}_{\mathrm{A}}$ the final form of the decoupler becomes

$$\boldsymbol{D}_{\mathrm{U}} = \left(\boldsymbol{G}_{\mathrm{D}} + \boldsymbol{G}_{\mathrm{A}}\right)^{-1} \boldsymbol{G}_{\mathrm{D}} = \boldsymbol{G}^{-1} \boldsymbol{G}_{\mathrm{D}} \tag{50}$$

Using the compensator the decoupling is obtained as

$$\boldsymbol{G}\,\boldsymbol{D}_{\mathrm{U}} = \left(\boldsymbol{G}_{\mathrm{D}} + \boldsymbol{G}_{\mathrm{A}}\right)\left(\boldsymbol{G}_{\mathrm{D}} + \boldsymbol{G}_{\mathrm{A}}\right)^{-1} \boldsymbol{G}_{\mathrm{D}} = \boldsymbol{G}_{\mathrm{D}} \tag{51}$$

Compared to the V-topology the effect of the main diagonal elements are still missing. It can be easily substituted if a diagonal element $\boldsymbol{V}_{\mathrm{D}}$ is serially connected to the compensator $\boldsymbol{D}_{\mathrm{U}}$. This effect is illustrated on the left side of Fig. 6 between the variables $\boldsymbol{e}$ and $\boldsymbol{c}$. This means at the same time that the relation between the two compensators can be simply written as

$$\boldsymbol{G}_{\mathrm{V}} = \boldsymbol{G}_{\mathrm{U}}\,\boldsymbol{V}_{\mathrm{D}} = \boldsymbol{G}^{-1} \boldsymbol{G}_{\mathrm{D}}\boldsymbol{V}_{\mathrm{D}} \tag{52}$$

There is the following simple relationship between the V- and U-topology

$$\boldsymbol{V} = \boldsymbol{V}_{\mathrm{D}} + \boldsymbol{V}_{\mathrm{A}} = \boldsymbol{V}_{\mathrm{D}}\left(\boldsymbol{I} + \boldsymbol{V}_{\mathrm{D}}^{-1}\boldsymbol{V}_{\mathrm{A}}\right) = \boldsymbol{V}_{\mathrm{D}}\left(\boldsymbol{I} + \boldsymbol{U}_{\mathrm{A}}\right) = \boldsymbol{V}_{\mathrm{D}}\boldsymbol{U} \tag{53}$$

what explaines all the above reults.

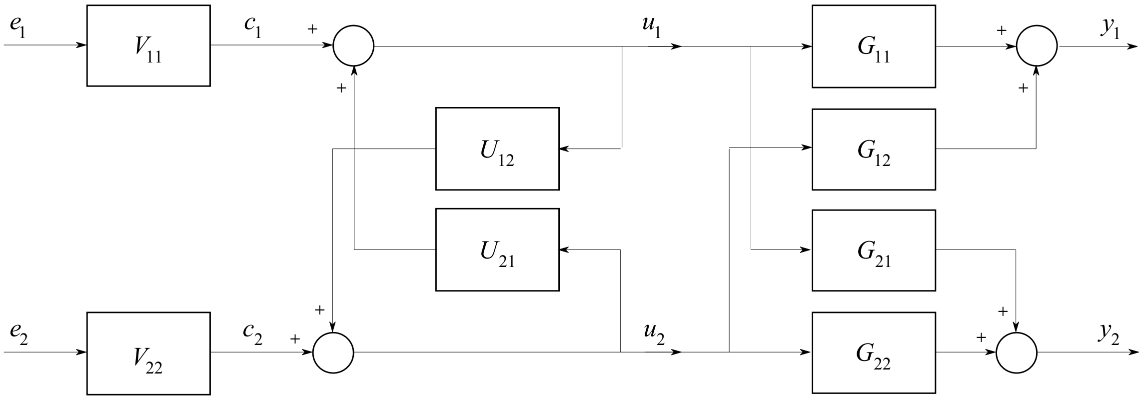

Figure 7. Joint block scheme of the decoupler and the process

The joint block scheme of the process and the decoupler of the U-topology is summarized in the Fig. 7. The cross-effects can be eliminated by the equations $G_{12} = -U_{21}G_{11}$ and $G_{21} = -U_{12}G_{22}$, whence the equations $U_{12} = -G_{21}/G_{22}$ and $U_{21} = -G_{12}/G_{11}$ are obtained for the decoupler. Due to the simplicity this method is widely used in the industrial practice of the decoupling by pairs.

This structure is beloved in the practical applications because the two inputs (V_{11} and U_{21} or V_{22} and U_{12}) of the summing elements allow to use standard PLC elements where the regulators (now V_{11} and V_{22}) appear together with the feed-forward elements (now U_{21} and U_{12}) what is usully the conventional tool of the classical solution of the noise compensation.

Besides the aboves, however, the decoupling can be performed by further simple topologies. The unity values of the diagonal elements can be used also for feed-forward structures. This method is used to be called *simple or simplified* decoupling method [9]. The corresponding S-topology of the decoupling block scheme is shown in Fig. 8.

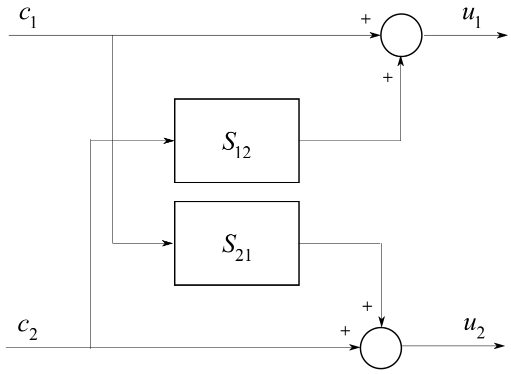

Figure 8. Block scheme of the decoupler of the S-topology

The basic relationship of the model can be written as

$$\boldsymbol{u}=\begin{bmatrix}u_1\\u_2\end{bmatrix}=\begin{bmatrix}1 & S_{12}\\S_{21} & 1\end{bmatrix}\begin{bmatrix}c_1\\c_2\end{bmatrix}=\left(\boldsymbol{I}+\boldsymbol{S}_A\right)\boldsymbol{c} \tag{54}$$

Introduce the following notation for the inverse of the process

$$\boldsymbol{G}^{-1}=\left(\boldsymbol{G}_{\mathrm{D}}+\boldsymbol{G}_{\mathrm{A}}\right)^{-1}=\bar{\boldsymbol{G}}_{\mathrm{D}}+\bar{\boldsymbol{G}}_{\mathrm{A}} \tag{55}$$

Let $\boldsymbol{S}_{\mathrm{A}}=\bar{\boldsymbol{G}}_{\mathrm{A}}\bar{\boldsymbol{G}}_D^{-1}$ be, then

$$\left(\boldsymbol{I}+\boldsymbol{S}_A\right)=\boldsymbol{I}+\bar{\boldsymbol{G}}_{\mathrm{A}}\bar{\boldsymbol{G}}_D^{-1}=\left(\boldsymbol{I}+\bar{\boldsymbol{G}}_{\mathrm{A}}\bar{\boldsymbol{G}}_D^{-1}\right)\bar{\boldsymbol{G}}_{\mathrm{D}}\bar{\boldsymbol{G}}_D^{-1}=\left(\bar{\boldsymbol{G}}_{\mathrm{D}}+\bar{\boldsymbol{G}}_{\mathrm{A}}\right)\bar{\boldsymbol{G}}_D^{-1}=\boldsymbol{G}^{-1}\bar{\boldsymbol{G}}_D^{-1} \tag{56}$$

Using the S-compensator the decoupling becomes

$$\boldsymbol{G}\boldsymbol{G}^{-1}\bar{\boldsymbol{G}}_D^{-1}=\bar{\boldsymbol{G}}_D^{-1} \tag{57}$$

Thus the decoupling is fulfilled but there are very complicated transfer functions in the diagonals, namely the reciprocals of the main diagonal of $\boldsymbol{G}^{-1}$.

It is worth noting that the decouplers of feedback topology are welcome in sampled time applications because the actuator signal can be easily computed and programmed using (44) from the following expression

$$\boldsymbol{u}=\boldsymbol{V}_{\mathrm{D}}\boldsymbol{e}-\boldsymbol{V}_{\mathrm{D}}\boldsymbol{V}_{\mathrm{A}}\boldsymbol{u}=\boldsymbol{V}_{\mathrm{D}}\left(\boldsymbol{e}-\boldsymbol{V}_{\mathrm{A}}\boldsymbol{u}\right)=\boldsymbol{G}_{\mathrm{D}}^{-1}\left(\boldsymbol{e}+\boldsymbol{G}_{\mathrm{A}}\boldsymbol{u}\right) \tag{58}$$

4. Decoupling control using YOULA-parametrized *MIMO* regulators

The *YP*-parametrized *MIMO* regulator, introduced in Section 2, makes also possible to solve the decoupling problem. The real advantage of this approach is that it is clearly observable whether the decoupling is possible or not.

According to (17) and choosing $\boldsymbol{G}_{\mathrm{r}} = \mathbf{I}$ and $\boldsymbol{G}_{\mathrm{n}} = \mathbf{I}$, the overall transfer characteristic of the closed system obtained by YOULA-parametrization for *MIMO* systems has the form

$$\boldsymbol{y} = \boldsymbol{P}_{-}\boldsymbol{R}_{\mathrm{r}}\,\boldsymbol{y}_{\mathrm{r}} + \left(\mathbf{I} - \boldsymbol{P}_{-}\boldsymbol{R}_{\mathrm{n}}\right)\boldsymbol{y}_{\mathrm{n}} = \boldsymbol{y}_{\mathrm{t}} + \boldsymbol{y}_{\mathrm{d}} \tag{59}$$

It is well seen that if the invariant *MIMO* process factor $\boldsymbol{P}_{-}$ is non-diagonal, then it is impossible to apply decoupling regulator. If $\boldsymbol{P}_{-}$ is diagonal or $\boldsymbol{P}_{-} = \mathbf{I}$, then choosing diagonal $\boldsymbol{R}_{\mathrm{r}}$ or $\boldsymbol{R}_{\mathrm{n}}$ [8], [9], the tracking and noise rejection decoupling can be performed. If $\boldsymbol{P}_{-}$ is diagonal, then the diagonal inner matrix filters $\boldsymbol{G}_{\mathrm{r}}$ or $\boldsymbol{G}_{\mathrm{n}}$ can also be applied for the optimal compensation of the invariant factors. In the case of diagonal reference models providing decoupling, the design of the main diagonal elements of the inner filters is completely the same as in the optimization methods shown for scalar (*SISO*) systems [6].

5. Decoupling examples

Example 1.
Consider a very simple *MIMO* process, whose *TFM* is $\boldsymbol{P}(s) = \mathcal{B}(s)/\mathcal{A}(s)$, i.e.,

$$\boldsymbol{P}(s) = \begin{bmatrix} \dfrac{1}{1+s} & \dfrac{1}{1+2s} \\ 0 & \dfrac{1}{1+4s} \end{bmatrix} = \frac{1}{(1+s)(1+2s)(1+4s)} \begin{bmatrix} (1+2s)(1+4s) & (1+s)(1+4s) \\ 0 & (1+s)(1+2s) \end{bmatrix} \tag{60}$$

Choose such reference models what can perform both the speeding up and decoupling design goals

$$\boldsymbol{R}_{\mathrm{n}}(s) = \frac{1}{\mathcal{A}_{\mathrm{n}}(s)}\mathcal{B}_{\mathrm{n}}(s) = \frac{1}{(1+0.5s)}\begin{bmatrix} 1 & 0 \\ 0 & 1 \end{bmatrix} = \frac{1}{(1+0.5s)}\mathbf{I} \tag{61}$$

After the calculations of (25) the following regulator is obtained

$$\boldsymbol{C}(s) = \begin{bmatrix} \dfrac{1+s}{0.5s} & -\dfrac{(1+s)(1+4s)}{0.5s(1+2s)} \\ 0 & \dfrac{1+4s}{0.5s} \end{bmatrix} \tag{62}$$

whose elements contain signal forming of *PI* and *PID* character.

Example 2.
Investigate now a DT process where the impulse *TFM* of the process is

$$\boldsymbol{G}(z) = \begin{bmatrix} \dfrac{0.5z^{-1}}{1-0.5z^{-1}} & \dfrac{0.2z^{-1}}{1-0.8z^{-1}} \\ 0 & \dfrac{z^{-1}-0.5z^{-2}}{1-1.7z^{-1}+0.2z^{-1}} \end{bmatrix} \tag{63}$$

Apply again the speeding up and decoupling design goals using the following reference model

$$
\boldsymbol{R}_{\mathrm{n}}(z)=\begin{bmatrix} \dfrac{0.8z^{-1}}{1-0.2z^{-1}} & 0 \\ 0 & \left(\dfrac{0.9z^{-1}}{1-0.1z^{-1}}\right)^2 \end{bmatrix}=\frac{\begin{bmatrix} 0.8z^{-1}\left(1-0.1z^{-1}\right)^2 & 0 \\ 0 & \left(0.9z^{-1}\right)^2\left(1-0.2z^{-1}\right) \end{bmatrix}}{\left(1-0.2z^{-1}\right)\left(1-0.1z^{-1}\right)^2} \tag{64}
$$

After the calculations given by (25), the impulse *TFM* of the obtained matrix regulator is

$$
\boldsymbol{C}(z)=\begin{bmatrix} C_{11}(z) & C_{12}(z) \\ C_{21}(z) & C_{22}(z) \end{bmatrix} \tag{65}
$$

where

$$
C_{11}(z)=\frac{1.6\left(1-0.5z^{-1}\right)}{1-z^{-1}} \quad ; \quad C_{12}(z)=\frac{-0.32\left(1-1.7z^{-1}+0.2z^{-2}\right)}{\left(1-z^{-1}\right)\left(1-0.8z^{-1}\right)} \tag{66}
$$

$$
C_{21}(z)=0 \quad ; \quad C_{22}(z)=\frac{0.81z^{-1}\left(1-1.7z^{-1}+0.2z^{-2}\right)}{\left(1-z^{-1}\right)\left(1+0.8z^{-1}\right)\left(1-0.5z^{-1}\right)} \tag{67}
$$

All elements of the regulator can be realized what is the consequence of the specially chosen reference model *TFM*. Since all non-trivial elements of $\boldsymbol{R}_{\mathrm{n}}$ have unity gain, therefore the scalar regulators have integrating character (i.e., all elements have the pole $z=1$).

Example 3.
An aircraft obviously has a very complex dynamics [1], [10], [13], which can be described by many state, input and/or output variables. Experts states that the vital lateral dynamics, however, can be described by relatively simple models which have four state variables and two major input signals. The input variables are the aileron δ_{a} and the rudder δ_{r}. For the small changes $\Delta\delta_{\mathrm{a}}$ and $\Delta\delta_{\mathrm{r}}$ in the vicinity of a working point we can introduce the following input vector

$$
\boldsymbol{u}=\left[\Delta\delta_{\mathrm{a}} \quad \Delta\delta_{\mathrm{r}}\right]^{\mathrm{T}} \tag{68}
$$

so the next state equation well approaches the dynamics [10], [13]

$$
\begin{aligned}
\dot{\boldsymbol{x}}&=\begin{bmatrix} Y_\beta & (\approx 0) & (\approx -1) & \dfrac{g}{V} \\ L_\beta & L_p & L_r & 0 \\ N_\beta & N_p & N_r & 0 \\ 0 & 1 & 0 & 0 \end{bmatrix}\boldsymbol{x}+\begin{bmatrix} 0 & Y_{\delta_{\mathrm{r}}} \\ L_{\delta_{\mathrm{a}}} & L_{\delta_{\mathrm{r}}} \\ N_{\delta_{\mathrm{a}}} & N_{\delta_{\mathrm{r}}} \\ 0 & 0 \end{bmatrix}\boldsymbol{u}=\mathbf{A}\,\boldsymbol{x}+\mathbf{B}\,\boldsymbol{u} \\
\boldsymbol{y}&=\mathbf{C}\,\boldsymbol{x}
\end{aligned} \tag{69}
$$

Here $\mathbf{A}$ and $\mathbf{B}$ contain the so-called dimensional derivatives typical for a given aircraft. The subscripts δ_{a} and δ_{r} refer to the aileron and rudder input, respectively. Introduce the following variables: the sideslip angle β, the roll rate p, the yaw rate r and the roll angle ϕ.

The small changes of the above variables produce the elements of the state vector, i.e.,

$$\boldsymbol{x} = \begin{bmatrix} \Delta\beta & \Delta p & \Delta r & \Delta\phi \end{bmatrix}^{\mathrm{T}} \tag{70}$$

The output variables depend on the selection of the structure of matrix $\mathbf{C}$. The following special selection, for example,

$$\boldsymbol{C} = \begin{bmatrix} 0 & 1 & 0 & 0 \\ 0 & 0 & 0 & 1 \end{bmatrix} \tag{71}$$

means that the output variables are the roll rate p and the roll angle ϕ, i.e., for their small changes

$$\boldsymbol{y} = \begin{bmatrix} \Delta p & \Delta\phi \end{bmatrix}^{\mathrm{T}} \tag{72}$$

It is an interesting task to design a simple decoupling regulator in order to reach the independent regulation of the roll rate and roll angle, or other selected output variables. The parameter matrices of the above state equation are available for different types of aircrafts in the literature. First choose an aircraft where this model is stable. A possible model according to [12] is

$$\begin{aligned}\dot{\boldsymbol{x}} &= \begin{bmatrix} -0.099593 & 0 & -1 & 0.1056796 \\ -1.700982 & -1.184647 & 0.223908 & 0 \\ 0.407420 & -0.056276 & -0.188010 & 0 \\ 0 & 1 & 0 & 0 \end{bmatrix} \boldsymbol{x} + \begin{bmatrix} 0 & 0.740361 \\ 0.531304 & 0.049766 \\ 0.005685 & -0.106592 \\ 0 & 0 \end{bmatrix} \boldsymbol{u} = \\ &= \mathbf{A}\boldsymbol{x} + \mathbf{B}\boldsymbol{u}\end{aligned} \tag{73}$$

From the eigenvalues $\{-0.0603 + 0.7555i; -0.0603 - 0.7555i; -1.3198; -0.0319\}$ of the matrix $\mathbf{A}$, two is complex conjugate and one is very slow. Let now the output variables be the sideslip angle β and the yaw rate r, i.e.,

$$\boldsymbol{y} = \begin{bmatrix} \Delta\beta & \Delta r \end{bmatrix}^{\mathrm{T}} \tag{74}$$

This task can be solved by the choice

$$\mathbf{C} = \begin{bmatrix} 1 & 0 & 0 & 0 \\ 0 & 0 & 1 & 0 \end{bmatrix} \tag{75}$$

To the decoupling choose the diagonal reference models

$$\boldsymbol{R}_{\mathrm{n}}(s) = \frac{1}{\mathcal{A}_{\mathrm{n}}(s)} \mathcal{B}_{\mathrm{n}}(s) = \frac{1}{(1+0.5s)} \begin{bmatrix} 1 & 0 \\ 0 & 1 \end{bmatrix} = \frac{2}{s+2} \mathbf{I} = \boldsymbol{R}_{\mathrm{r}} \tag{76}$$

Using (25) we can compute the decoupling regulator as

$$\mathcal{C}(s)=\begin{bmatrix}\mathcal{C}_{11}(s) & \mathcal{C}_{12}(s)\\ \mathcal{C}_{21}(s) & \mathcal{C}_{22}(s)\end{bmatrix} \tag{77}$$

where

$$\mathcal{C}_{11}(s)=\frac{50.6501(s-2.862)(s+1.383)(s-0.04035)}{s(s+3.687)(s+3.687)} \tag{78}$$

$$\mathcal{C}_{12}(s)=\frac{351.803(s+1.154)(s+0.3676)(s-0.004883)}{s(s+3.687)(s+3.687)} \tag{79}$$

$$\mathcal{C}_{21}(s)=\frac{2.7014(s-3.79)(s-1.15)(s+0.9645)}{s(s+3.687)(s+3.687)} \tag{80}$$

$$\mathcal{C}_{22}(s)=\frac{2.7014(s-14.08)(s+0.1335)}{s(s+3.687)(s+3.687)} \tag{81}$$

It can be checked by simple calculations that the overall characteristic of the closed system is

$$\boldsymbol{y}=\begin{bmatrix}\Delta\beta\\ \Delta r\end{bmatrix}=\frac{2}{s+2}\mathbf{I}\begin{bmatrix}\Delta\delta_{\mathrm{a}}\\ \Delta\delta_{\mathrm{r}}\end{bmatrix}+\frac{2}{s+2}\mathbf{I}\,\boldsymbol{y}_{\mathrm{n}} \tag{82}$$

i.e., the decoupling is realized both for tracking and noise rejection. Each element of the *MIMO* regulator is realizable integrating regulator with third order transfer functions. Of course, depending on the feature of the task, different reference models can be chosen for $\boldsymbol{R}_{\mathrm{r}}$ and $\boldsymbol{R}_{\mathrm{n}}$.

On the basis of [13], the state equation of an unstable aircraft can be obtained by linearization around the working point

$$\dot{\boldsymbol{x}}=\begin{bmatrix}-0.05 & -0.003 & -0.98 & 0.2\\ -1.0 & -0.75 & 1.0 & 0\\ 0.3 & -0.3 & -0.15 & 0\\ 0 & 1 & 0 & 0\end{bmatrix}\boldsymbol{x}+\begin{bmatrix}0 & 0\\ 1.7 & -0.2\\ 0.3 & -0.6\\ 0 & 0\end{bmatrix}\boldsymbol{u}=\mathbf{A}\,\boldsymbol{x}+\mathbf{B}\,\boldsymbol{u} \tag{83}$$

where the relative gain for the aileron and rudder are $g_1=1.0$ and $g_2=\delta_{\mathrm{r}}/\delta_{\mathrm{a}}$.

The dynamic model of most of the aircrafts for the above state variables, however, is unstable. The YOULA-parametrization based regulators can be applied only for stable processes. The solution may the usual two-step method, where first an inner control loop is applied to stabilize the system.

The eigenvalues of the matrix $\mathbf{A}$ are $\{-0.0035\pm 0.8834i; -0.9821; -0.0391\}$. The two complex conjugate poles and one of the real poles are stable, the other pole is unstable. This latter one corresponds to the instability of the so-called spiral dynamics. Different types of stabilizing regulators can be applied. The simplest case when the stabilization is solved by state feedback. Choose the following design poles: $\{-0.0035\pm 0.8834i; -0.9821; -0.0391\}$, i.e., mirror the unstable pole on the complex axis. This pole assigning task can be solved by the following state feedback matrix

$$\boldsymbol{K}=\begin{bmatrix}-0.5606 & -0.3848 & 0.5529 & 0.5071\\ -0.7622 & 0.2099 & -1.0143 & 0.6824\end{bmatrix} \tag{84}$$

Let the output variables be the sideslip β and roll angle ϕ, i.e.,

$$\boldsymbol{y}=\left[\Delta\beta \quad \Delta\phi\right]^{\mathrm{T}} \tag{85}$$

and the corresponding control matrix is

$$\boldsymbol{C}=\begin{bmatrix}1 & 0 & 0 & 0\\ 0 & 0 & 0 & 1\end{bmatrix} \tag{86}$$

Similarly to the previous case the elements of the *MIMO* regulator are

$$\mathcal{C}_{11}(s)=\frac{0.42517\left(s^2+0.5416s+0.6217\right)}{s} \tag{87}$$

$$\mathcal{C}_{12}(s)=\frac{1.2513\left(s^2-0.0332s+0.7768\right)}{s} \tag{88}$$

$$\mathcal{C}_{21}(s)=\frac{3.6139(s+0.8423)(s+0.107)}{s} \tag{89}$$

$$\mathcal{C}_{22}(s)=\frac{0.63584\left(s^2-1.395s+1.124\right)}{s} \tag{90}$$

Here we got *PID* regulators in each element of the matrix regulator. The overall characteristic of the closed system is

$$\boldsymbol{y}=\begin{bmatrix}\Delta\beta\\ \Delta\phi\end{bmatrix}=\frac{2}{s+2}\mathbf{I}\begin{bmatrix}\Delta\delta_{\mathrm{a}}\\ \Delta\delta_{\mathrm{r}}\end{bmatrix}+\frac{2}{s+2}\mathbf{I}\,\boldsymbol{y}_{\mathrm{n}} \tag{91}$$

References

[1] Allerton, D. Principles of Flight Simulation, John Wiley & Sons, 2009.

[2] Bányász, Cs. and L. Keviczky. Youla-parametrized MIMO controller design for stable multivariable processes. Int. Conf. on Control CONTROL’2010, Coventry, UK, 2010, pp. 126-131.

[3] Etkin, B. and L.D. Reid. Dynamics of Flight Stability and Control, John Wiley & Sons, 1996.

[4] Ghosh, A. and S.K. Das. Open-loop decoupling of MIMO plants, IEEE Trans. on Aut. Contr., 2009, 54, August, pp. 1977-1981.

[5] Harold, L.W. Inverted decoupling – a neglected technique. IEEE Trans. Aut. Control, 1997, Vol. AC-36, 1, pp. 3-10.

[6] L. Keviczky and Cs. Bányász (2001). Iterative identification and control design using KB-parametrization, In: Control of Complex Systems, Eds: K.J. Åström, P. Albertos, M. Blanke, A. Isidori, W. Schaufelberger and R. Sanz, Springer, pp. 101-121.

[7] Keviczky, L. and Cs. Bányász. Youla-parametrized controllers for stable multivariable processes. Acta Technica Jaurinensis, 2010, 3(2), pp. 187-196.

[8] Keviczky, L. and Cs. Bányász. Decoupling autopilot MIMO controller design. 31.

IASTED Conf. on Modelling, Identification and Control MIC'11, 2011, Innsbruck, A.
[9] Keviczky, L. and Cs. Bányász. MIMO controller design for decoupling aircraft lateral dynamics, 9th IEEE Conf. on Control and Automation, ICCA'11, Santiago, Chile, 2011, pp. 1079-1084.
[10] McLean, D. Automatic Flight Control Systems, Prentice Hall, 1990.
[11] Maciejowski, J.M. Multivariable Feedback Design, Addison Wesley, 1989.
[12] Morari, M. and E. Zafiriou. Robust Process Control. Prentice-Hall, London, 1989.
[13] Nelson, R.C., Flight Stability and Automatic Control, WCB/McGraw-Hill, 1998.
[14] Qing-Guo Wang. Decoupling Control. Springer, 2003.
[15] Skogestad, S. and I. Poslethwaite. Multivariable Feedback Control: Analysis and Design, Wiley, second edition, 2005.

This work was supported in part by the Control Engineering Research Group of the HAS, at the Budapest University of Technology and Economics and by the project TAMOP 4.2.2.A-11/1/KONV-2012-2012, at the Széchenyi University of Győr.